Separation Science and Technology
Publication details, including instructions for authors and subscription information:
http://www.informaworld.com/smpp/title~content=t713708471

Isothermal Vapor-Liquid Equilibrium of Ethanol-Water Mixtures Acetone-Ethanol Mixtures Inside Capillary Porous Plates

Fahmi A. Abu Al-Rub[a]; Ravindra Datta[b]
[a] DEPARTMENT OF CHEMICAL ENGINEERING, JORDAN UNIVERSITY OF SCIENCE AND TECHNOLOGY, IRBID, JORDAN [b] DEPARTMENT OF CHEMICAL ENGINEERING, WORCESTER POLYTECHNIC INSTITUTE, WORCESTER, MASSACHUSETTS, USA

Online publication date: 11 September 2000

To cite this Article Al-Rub, Fahmi A. Abu and Datta, Ravindra(2000) 'Isothermal Vapor-Liquid Equilibrium of Ethanol-Water Mixtures Acetone-Ethanol Mixtures Inside Capillary Porous Plates', Separation Science and Technology, 35: 14, 2203 — 2225
To link to this Article: DOI: 10.1081/SS-100102098
URL: http://dx.doi.org/10.1081/SS-100102098

SEPARATION SCIENCE AND TECHNOLOGY, **35**(14), pp. 2203–2225, 2000

Isothermal Vapor–Liquid Equilibrium of Ethanol–Water Mixtures + Acetone–Ethanol Mixtures Inside Capillary Porous Plates

FAHMI A. ABU AL-RUB*
DEPARTMENT OF CHEMICAL ENGINEERING
JORDAN UNIVERSITY OF SCIENCE AND TECHNOLOGY, IRBID, JORDAN

RAVINDRA DATTA
DEPARTMENT OF CHEMICAL ENGINEERING
WORCESTER POLYTECHNIC INSTITUTE, WORCESTER, MASSACHUSETTS, USA

ABSTRACT

Isothermal vapor–liquid equilibrium (VLE) of ethanol–water mixtures at different temperatures and the isothermal VLE of acetone–ethanol mixtures at 305.15 K were experimentally measured in three different macroporous plates: a 13.5-μm pore diameter sintered stainless steel plate, a 30-μm pore diameter porous carbon plate, and a 30-μm pore diameter porous Teflon plate. The experimental results showed that the VLE of the ethanol–water system in the porous sintered stainless steel plate was dramatically altered, and the azeotropic point was shifted from ethanol mole fraction of 0.90 to > 0.99. However, there was no significant effect of this plate on the acetone–ethanol system. The effect of either the porous Teflon plate or the porous carbon plate on the VLE was insignificant for both systems. These results show that for substantial alteration of the VLE binary mixtures, two conditions are required: the liquid components must be of different polarity, and the porous plate should possess high polarization.

Key Words. Ethanol; Porous plates; Capillarity; Activity coefficients azeotrope

* To whom correspondence may be addressed.

INTRODUCTION

Distillation is the most common separation process used in the chemical industries. However, in many cases the vapor–liquid equilibrium (VLE) of a given system imposes thermodynamics constraints on using distillation for separating the components of the system. One thermodynamics constraint is the presence of azeotropes. For these cases special techniques such as extractive and azeotropic distillation can be used. For binary mixtures, a third component is added to alter the vapor–liquid equilibrium of the binary mixture; thus efficient separation can be achieved. However, this adds substantially to the cost, because additional columns are usually required to remove and recycle the component added. As a result, alternative processes such as adsorption and pervaporation are being considered, and in some cases have replaced azeotropic or extractive distillation, e.g., in ethanol–water separation (1–3).

An innovative alternative separation method, called capillary distillation, was proposed by Yeh et al. (4–6) and later Abu Al-Rub et al. (7) and Abu Al-Rub and Datta (8–10) to separate binary mixtures with an azeotropic point. Capillary distillation is a new method that utilizes the surface forces of the solids and the consequent intermolecular interactions between the solid and liquids, which in turn alter the intermolecular interactions among the solution components, thus altering the VLE. Because of the porous solid–liquid interactions, a layer with different physicochemical properties from those in the bulk phases may be created next to the solid surface. Another interaction, in principle, that is responsible for alteration of the VLE in a porous material is the interface curvature, as given by the well-known Kelvin equation (4–10)

$$\ln\left(\frac{p^{r}_{v,o}}{p^{\infty}_{v,o}}\right) = -\frac{2\sigma_o \tilde{V}_{l,o}}{rRT} \tag{1}$$

However, the studies of Yeh et al. (4–6), Abu Al-Rub et al. (7), Abu Al-Rub and Datta (8–10), and Wong (11) show that the Kelvin effect is negligible for pores of radii > 0.1 μm. Abu Al-Rub and Datta (9–10) analyzed the VLE in porous media using a molecular thermodynamics approach. They concluded that the main factor affecting the alteration of VLE in porous media is the intermolecular interaction between the liquids and the solid.

This study investigates, experimentally and theoretically, the VLE of binary mixtures inside capillary porous plates. A generalized framework of VLE in the presence of arbitrary external fields was developed and applied to the VLE of binary mixtures inside porous materials to account for the influence of long-range surface forces exerted by the proximate solid on the liquid. The VLE of two binary mixtures, one consisting of components of different polarity, e.g., ethanol–water system, the other containing components of similar polarity, ethanol–acetone system, in porous plates of different polarization were exper-

imentally studied to elucidate the effect of material properties on the alteration of VLE.

THEORY

Vapor–Liquid Equilibrium in the Presence of External Fields

Abu Al-Rub and Datta (9–10) studied the equilibrium criteria for a heterogeneous multicomponent system containing π phases and n chemical species that were under the influence of l external force fields. These fields may be externally imposed or may be a long-range surface acting across the system boundaries. The condition for equilibrium then is (9–10)

$$\psi_{i1} = \psi_{i2} = \ldots \psi_{i\alpha} = \ldots = \psi_{i\pi} \tag{2}$$

where the generalized physicochemical potential becomes defined by

$$\psi_{i\alpha} \equiv \mu_{i\alpha} + \sum_{b=1}^{l} \Psi_{ib\alpha} \otimes \bar{\zeta}_{ib\alpha} \tag{3}$$

where the last term on the right-hand side denotes the additional term for the work done against the system by increasing $d\zeta_{ib}^{\alpha}$ infinitesimally. Here ζ_{ib}^{α} is an extensive parameter corresponding to the intensive parameter Ψ_{ib}^{α}, which characterizes the external field b acting on phase α and may be species specific. In Eq. (3), the symbol $\otimes$ denotes the appropriate scalar product dependent on the tensorial character of Ψ and ζ. For instance, for the system under the influence of long-range surface forces considered here, Ψ_b includes Ψ_D, Ψ_K, Ψ_L and Ψ_O referring, respectively, to the Debye, Keesom, London, and other molecular interactions, whereas $\zeta_b = A^{\alpha\beta}$, i.e., the molar interfacial area between phase α and phase β. Equation (3) further assumes spatial uniformity of the external field in the system of interest. If this is not the case, then integration over the system volume V is required. Equation (3) is similar to the usual criterion for phase equilibrium, i.e., in the absence of external fields, when it reduces to $\mu_{i1,o} = \mu_{i2,o} = \ldots = \mu_{i\alpha,o} = \ldots = \mu_{i\pi,o}$, because then $\psi_{i\alpha} = \mu_{i\alpha} = \mu_{i\alpha,o}$.

Abu Al-Rub and Datta (10) showed that the criterion for VLE in the presence of external fields is given by

$$y_i p = \gamma_i x_i p_{iv} \qquad i = 1,2, \ldots ,n \tag{4}$$

Equation (4) is of a form equivalent to that in the absence of external fields, when it reduces to

$$y_i p_o = \gamma_{i,o} x_i p_{iv,o} \qquad i = 1,2, \ldots, n \tag{5}$$

i.e., the vapor pressure, the total pressure, and the activity coefficients are all, in general, affected by the presence of external fields.

The distribution coefficient of the species i

$$K_i \equiv \frac{y_i}{x_i} = \frac{\gamma_i p_{iv}}{p} \tag{6}$$

Furthermore, relative volatility is

$$\alpha_{ij} \equiv \frac{K_i}{K_j} = \frac{y_i/x_i}{y_j/x_j} = \frac{\gamma_i p_{iv}}{\gamma_j p_{jv}} \tag{7}$$

The distribution coefficient at a given temperature in the presence of external fields may next be related to that in their absence

$$\frac{K_i}{K_{i,o}} = \frac{\gamma_i p_{iv} p_o}{\gamma_{i,o} p_{iv,o} p} \qquad i = 1,2, \ldots, n \tag{8}$$

Similarly, the analogous ratio of relative volatility

$$\frac{\alpha_{ij}}{\alpha_{ij,o}} = \left(\frac{\gamma_i}{\gamma_{i,o}}\right)\left(\frac{\gamma_{j,o}}{\gamma_j}\right)\left(\frac{p_{iv}}{p_{iv,o}}\right)\left(\frac{p_{jv,o}}{p_{jv}}\right) \qquad i = 1,2, \ldots, n \tag{9}$$

Thus, using the above relations, the activity coefficient can be determined from experimental values for the liquid and vapor composition and the vapor pressure and total pressure in the presence of external fields. Alternatively, if predictive relationships are available for the activity coefficients and the vapor pressures in the presence of external fields, the distribution coefficient or the relative volatility in the presence of external fields may be predicted, as discussed next.

Activity Coefficients in the Presence of External Fields

The presence of external fields may lead to a further deviation from the ideality of a liquid mixture because of induced polarization and altered orientation, etc. The partial molar excess Gibbs free energy in the presence of external fields is related to the corresponding activity coefficients by

$$RT \ln\gamma_i = \overline{G}_i^E \equiv \left(\frac{\partial G^E}{\partial n_i}\right)_{T,p,n_{j\neq i}} \tag{10}$$

where γ_i is the activity coefficient of i in the presence of external fields. For the entire solution, in molar form

$$\tilde{G}^E = \sum_{i=1}^{n} x_i \overline{G}_i^E = RT \sum_{i=1}^{n} x_i \ln\gamma_i \tag{11}$$

It is assumed that the excess Gibbs free energy in the presence of external force fields is a sum of two contributions, an intrinsic contribution, $\overline{G}_{i,o}^E$, and a

contribution resulting from the effects of external fields, $\overline{G}^E_{i,F}$

$$\overline{G}^E_i = \overline{G}^E_{i,o} + \overline{G}^E_{i,F} \tag{12}$$

Using Eq. (10) in Eq. (12)

$$\ln\gamma_i = \ln\gamma_{i,o} + \ln\gamma_{i,F} \tag{13}$$

or

$$\gamma_i = \gamma_{i,o}\gamma_{i,F} \qquad i = 1,2, \ldots ,n \tag{14}$$

Thus, from experimental measurements of the activity coefficients in the absence and in the presence of external fields, the effect of external fields on activity coefficients can be discerned.

Use of Eq. (12) in Eq. (11) further gives

$$\tilde{G}^E = \sum_{i=1}^{n} x_i(\overline{G}^E_{i,o} + \overline{G}^E_{i,F}) = \sum_{i=1}^{n} x_i\overline{G}^E_{i,o} + \sum_{i=1}^{n} x_i\overline{G}^E_{i,F} \tag{15}$$

Thus

$$\tilde{G}^E = \tilde{G}^E_o + \tilde{G}^E_F \tag{16}$$

and

$$\frac{\tilde{G}^E}{RT} = \sum_{i=1}^{n} x_i \ln(\gamma_{i,o}\gamma_{i,F}) \tag{17}$$

which can be used to obtain the excess Gibbs energy in the presence or absence of external fields from the corresponding activity coefficients determined from experiments, as discussed below.

Vapor Pressure in Capillary Porous Plates

Abu Al-Rub and Datta (9) showed that the vapor pressure in capillary porous media is given by (9)

$$\ln\left(\frac{p_{iv}}{p_{iv,o}}\right) = C^E_i - \frac{\Delta H^E_{ivl}}{RT} - \frac{2\sigma_{il}\tilde{V}^l_i}{rRT} \tag{18}$$

where $C^E_i \equiv C_i - C_{i,o}$, C_i is the constant of integration in the Clapeyron equation, $\ln p_{iv} = C_i - \Delta\tilde{H}_{ivl}/RT$, whereas $C_{i,o}$ is the constant in the corresponding equation in the absence of external fields, $\ln p_{iv,o} = C_{i,o} - \Delta\tilde{H}_{ivl,o}/RT$ (9). The excess enthalpy due to the external fields, $\Delta\tilde{H}^E_{ivl} \equiv \Delta\tilde{H}_{ivl} - \Delta\tilde{H}_{ivl,o}$. It was, however, concluded by Abu Al-Rub and Datta (9–10) that the effect of curvature of the capillary porous plates of pore diameter larger than 6.5 μm is usually negligible. Although the study of Abu Al-Rub and Datta (9–10) was for two capillary porous plates, sintered stainless steel plates and porous carbon plates, similar results have been obtained by Wong (11) for different porous

plates with pore diameters less than 0.50 μm. The excess enthalpy of vaporization of pure liquid i resulting from these interactions was related by Abu Al-Rub and Datta (9) to the molar polarization and molar volume of both the liquid and the solid, as well as a characteristic constant for the porous solid by (9)

$$\frac{\Delta\tilde{H}^E_{ivl}}{RT} = \frac{\Delta\tilde{H}^E_{L,ivl}}{RT} + \kappa\left(\frac{\tilde{P}^l_i}{\tilde{V}^l_i}\right)\left\{\left(\frac{\tilde{P}^s}{\tilde{V}^s}\right) - \left(\frac{\tilde{P}^l_i}{\tilde{V}^l_i}\right)\right\} \tag{19}$$

which may frequently be linearized to (9)

$$\frac{\Delta\tilde{H}^E_{ivl}}{RT} \cong \frac{\Delta\tilde{H}^E_{L,ivl}}{RT} + \kappa_s\left(\frac{\tilde{P}^l_i}{\tilde{V}^l_i}\right) \tag{20}$$

where κ_s is a characteristic constant for the porous solid, $\Delta\tilde{H}^E_{L,vl}$ is the dispersion interaction contribution, which can be assumed to be constant. Thus, Eq. (20), or (19), along with Eq. (18), can be used to correlate the vapor pressure of pure liquids in porous plates.

Distribution Coefficient and Relative Volatility in Capillary Porous Plates

For the specific case of VLE in porous media, use of Eqs. (19) and (20) in Eq. (8) results in

$$\ln\frac{K_i}{K_{i,o}} = \ln\gamma_{i,F} + C^E_i - \frac{\Delta\tilde{H}^E_{L,ivl}}{RT} - \kappa_s\left(\frac{\tilde{P}_{il}}{\tilde{V}_{il}}\right) - \ln\left(\frac{p}{p_o}\right) \tag{21}$$

Similarly,

$$\ln\frac{\alpha_{ij}}{\alpha_{ij,o}} = \ln\frac{\gamma_{i,F}}{\gamma_{j,F}} + (C^E_i - C^E_j) - \frac{1}{RT}(\Delta\tilde{H}^E_{ivl} - \Delta\tilde{H}^E_{jvl}) \tag{22}$$

Using Eq. (20)

$$\ln\frac{\alpha_{ij}}{\alpha_{ij,o}} = \ln\frac{\gamma_{i,F}}{\gamma_{j,F}} + (C^E_i - C^E_j) - \frac{1}{RT}(\Delta\tilde{H}^E_{L,ivl} - \Delta\tilde{H}^E_{L,jvl}) - \kappa_s\left(\frac{\tilde{P}^l_i}{\tilde{V}^l_i} - \frac{\tilde{P}^l_j}{V^l_j}\right) \tag{23}$$

This equation shows that for liquids of similar polarity in a porous medium, even though the individual vapor pressure may be substantially affected, relative volatility may not be materially affected. Thus, disparate polarities are essential for substantial alteration of the relative volatility. Equation (23) may be somewhat further simplified by dropping the third term on its right-hand side, because it was shown that the London terms for different species in a given porous media are similar (9).

EXPERIMENTAL

Procedure

The VLE of binary mixtures in macroporous plates under isothermal conditions was experimentally measured using the static still method. The still consists of two Pyrex chambers with ground glass joints, between which the porous plate is mounted and sealed. The mixture solution, after being degassed, is charged into the lower chamber, while the upper chamber contains the vapor, the vapor–liquid interface being located within the porous plate. The apparatus has ports for evacuation, pressure measurement, liquid introduction, and sample withdrawal, and upon charging is placed in a thermostatically controlled constant-temperature air bath. A detailed description of the procedure and the still used to study vapor–liquid equilibria in capillary porous plates can be found elsewhere (4, 12).

The porous polar plates used in this study were sintered stainless steel plates with specifications listed in Table 1. These plates were air blown to remove any dust and then washed in a beaker containing acetone for 24 h. Next, the plates were dried in a vacuum then immersed in boiling distilled water for 8 h twice, using fresh water each time. The plates were then tested for cleanliness by using fresh distilled water and observing their ability to be wetted completely and instantly.

The porous nonpolar plates used in this study were porous carbon and Teflon plates with specifications listed in Table 2. These porous plates were prepared by machining them from a larger sheet of the same material. These plates were air blown to remove any dust and then washed with distilled water, then dried and immersed in 2-propanol for 1 h, then washed with water, dried, and put in sulfuric acid for 1 h. Then the plates were immersed in boiling distilled water for 8 h twice, using fresh water each time. The plates were then tested for perfect cleanliness.

TABLE 1
Specifications of Sintered Stainless Steel Plates

Manufacturer	Technetics Corporation
Product number	FM 1104
Plate thickness	4.9×10^{-5} m
Area density	439.2 kg/m^2
Median pore size	13 μm
Pore size range	7–72 μm
Tensile strength	4.136×10^9 N/m^2
Surface area	13,300 m^2/kg

TABLE 2
Specifications of Porous Carbon and Teflon Plates

	a. Porous carbon plate	b. Porous Teflon plate
Manufacturer	Union Carbide Corporation	Engineering Seal Products Inc.
Porosity	52%	52%
Plate thickness	4.9×10^{-5} m	4.9×10^{-5} m
Bulk density	1050 kg/m^3	30 μm
Median pore size	30 μm	
Flexural strength	2.76×10^8 N/m^2	
Compressive strength	4.136×10^8 N/m^2	

After the plates were prepared, they were mounted in the static apparatus. The apparatus was then closed, evacuated, and placed in the constant-temperature air bath. The maximum error in temperature measurement was estimated to be ±0.1 K. After equilibrium was reached (24 h), samples of the liquid and vapor were withdrawn for analysis by a Perkin Elmer Auto System Gas Chromatograph using a 6 ft, $\frac{1}{8}$ in, Porapak R column under isothermal conditions at 443.15 K. Calibration was done for each mixture used, and the accuracy of analysis was estimated to be within ±0.1%. The experiments were conducted with different feed compositions to cover the entire range between $x_1 = 0$ to 1.

Two different binary mixtures were studied: (i) ethanol(1)–water(2) system (ethanol was obtained from Midwest Grain Product, 200 proof), and (ii) acetone(1)–ethanol(2) system (acetone was obtained from Fisher with 99.7% purity). The first system has an azeotropic point and has components of distinctly different polarity, the relative permittivity at 298.15K being 24.55 and 78.5, respectively, whereas the second system has no azeotrope and components of similar polarity, with relative permittivity at 298.15 K of 20.75 and 24.55, respectively (13). Both systems were studied in both the porous plates; however, the first system was studied at three temperatures, i.e., 323.15, 328.15, and 333.15 K, whereas the second system was studied only at 305.15 K.

RESULTS AND DISCUSSION

VLE of Binary Mixtures in Capillary Porous Plates

The experimental isothermal VLE data for ethanol(1)–water(2) mixtures at 323.15 K with and without the porous plates are shown in Fig. 1 and presented in Table 3, while those for the acetone(1)–ethanol(2) system at 305.15 K are

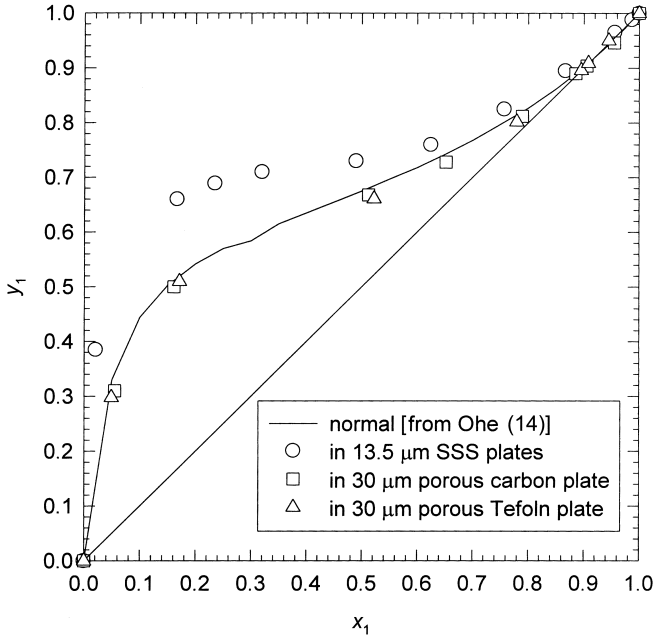

FIG. 1 $x_1 - y_1$ diagram (isothermal) for ethanol(1)–water(2) system at 323.15 K. The normal curve is from Ohe (14).

shown in Fig. 2 and presented in Table 4. Figure 1 shows that the VLE for the ethanol–water system in the sintered stainless plates is quite different from the normal VLE (14). It is seen that although the $x - y$ plot in either the porous Teflon or the porous carbon plate is very similar to the normal plot, that in the porous sintered stainless steel plate has been greatly altered. This is particularly evident at low ethanol concentrations, e.g., $x_1 < 0.5$. Although apparently less dramatic at higher concentrations, the shifting of the azeotropic point from $x_1 \cong 0.90$ to $x_1 > 0.99$ is very significant. The shifting of the azeotrope is more easily seen in Fig. 3, where the relative volatility of ethanol with respect to water at 323.15 K is plotted. Figure 3 shows that there is a substantial increase in the relative volatility of ethanol in the sintered stainless steel plate, the increase being about threefold the normal increase at low concentrations. Furthermore, it is clear that the azeotropic point in this case has shifted from $x_1 \cong 0.90$ to the neighborhood of $x_1 \to 1$. These results are similar to those obtained by Yeh et al. (4) and Wong (11). In the case of an ethanol–water system in porous carbon or Teflon plates, however, the change in the VLE is insignificant, with no discernible shift in the azeotropic point.

TABLE 3
Experimental Data of VLE of Ethanol–Water Mixtures

a. In 30-μm porous Teflon plate at 323.15 K

x_1	y_1	P (mm Hg)
0.0000	0.0000	86.2
0.0491	0.2980	122.1
0.1711	0.5104	159.2
0.5219	0.6610	193.9
0.7790	0.8021	202.3
0.8950	0.8960	207.4
0.9081	0.9089	208.7
0.9453	0.9500	209.1
1.0000	1.0000	208.1

b. In 30-μm porous carbon plate at 328.15 K

x_1	y_1	P (mm Hg)
0.0000	0.0000	87.5
0.0550	0.3100	125.1
0.1610	0.4999	157.9
0.5121	0.6601	193.6
0.6519	0.7199	201.4
0.7892	0.8121	204.9
0.8849	0.8887	208.5
0.9049	0.9041	208.8
0.9550	0.9462	209.0
1.0000	1.0000	208.5

c. In 13.5-μm sintered stainless steel plate at 323.15 K

x_1	y_1	P (mm Hg)
0.0211	0.3850	93.2
0.1670	0.6600	144.3
0.2349	0.6893	150.2
0.3321	0.7101	164.3
0.4900	0.7299	173.2
0.6247	0.7600	181.2
0.7570	0.8121	185.4
0.8670	0.8949	191.6
0.9560	0.9650	192.1
0.9870	0.9880	192.3

TABLE 3 Continued

d. In 13.5-μm sintered stainless steel plate at 328.15 K

x_1	y_1	P (mm Hg)
0.0200	0.3610	127.6
0.1511	0.6600	205.0
0.2899	0.7012	217.2
0.4010	0.7150	233.0
0.5981	0.7600	243.5
0.7011	0.8012	250.1
0.8446	0.8803	256.7
0.9040	0.9179	257.8
0.9400	0.9480	258.0
0.9810	0.9820	258.1

e. In 13.5-μm sintered stainless steel plate at 333.15 K

x_1	y_1	P (mm Hg)
0.0200	0.3601	150.1
0.2950	0.7000	260.1
0.4888	0.7280	277.0
0.5947	0.7521	285.2
0.7100	0.8022	292.4
0.7982	0.8413	298.0
0.9010	0.9172	307.1
0.9501	0.9580	308.5
0.9800	0.9810	310.2

Furthermore, for the acetone(1)–ethanol(2) system, it can be seen from Fig. 2 that there is no perceptible change in the $x - y$ plot for any of the porous plates.

These experimental results can be qualitatively rationalized as follows. As discussed above, the long-range surface forces exerted by the porous material have two effects: (a) they reduce the vapor pressure of each component, and (b) they alter the intermolecular interaction of the mixture components, thereby changing their activity coefficients. As discussed above, the vapor pressure reduction can be explained in terms of the excess enthalpy of vaporization in porous solids, which is a function of both the solid and the liquid polarization. Thus, Abu Al-Rub and Datta (9) showed that excess enthalpy of vaporization in porous sintered stainless steel is high, increasing directly with liquid polarity. However, the excess enthalpy of vaporization in nonpolar plates is relatively low and largely independent of the liquid polarity. Nonpo-

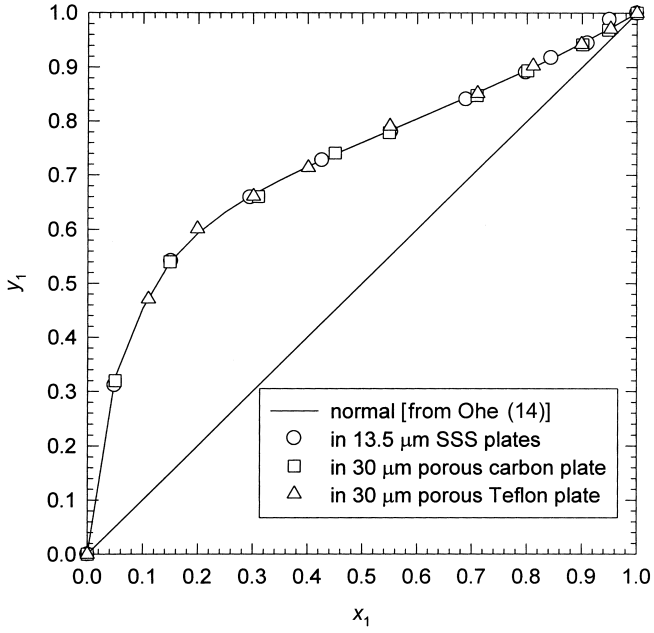

FIG. 2 $x_1 - y_1$ diagram (isothermal) for acetone(1)–ethanol(2) system at 305.15 K. The normal curve is from Ohe (14).

lar liquids have low excess enthalpy of vaporization that is relatively independent of the polarization of the porous material.

On the other hand, the variation of the activity coefficients depends on the change of intermolecular interactions of the mixture components and, hence, upon the *difference* between the effects of the porous material on individual components of the mixture. If it is assumed, for instance, on the basis of a linear free energy relation, that the excess partial molar Gibbs free energy change of a component due to external fields, $\overline{G}^E_{i,F}$, is proportional to its excess enthalpy change, $\Delta\tilde{H}_{ivl}$, then it can be seen that *both* dissimilar polarity of components along with a porous material of high polarization are required for any substantial alteration of the relative volatility. The ethanol–water system, has a considerable difference in the polarization of the mixture components; thus, the change in relative volatility is high in the porous sintered stainless steel plate, resulting in a shifting of the azeotrope, but not so in the porous carbon plate. For the acetone–ethanol system, however, it can be seen from Fig. 2 that there is no significant change in the $x - y$ plot in any of the porous plates. This is because acetone and ethanol have similar polarization, i.e., $\varepsilon_1 = 20.75$ and $\varepsilon_2 = 24.55$, respectively (13); thus the intermolecular interactions between the

TABLE 4
Experimental Data of VLE of Acetone–Ethanol Mixtures at 305.15 K

a. In 30-μm porous Teflon plate

x_1	y_1	P (mm Hg)
0.1101	0.4714	138.2
0.1988	0.6012	166.5
0.3012	0.6611	184.0
0.4012	0.7145	198.8
0.5501	0.7912	222.3
0.7102	0.8524	241.1
0.8109	0.9033	251.9
0.8988	0.9429	265.2
0.9521	0.9710	271.1

b. In 30-μm porous carbon plate

x_1	y_1	P (mm Hg)
0.0512	0.3211	106.3
0.1488	0.5401	154.2
0.3101	0.6600	188.5
0.4500	0.7409	211.4
0.5491	0.7703	223.3
0.7088	0.8479	245.3
0.8010	0.8916	255.6
0.9099	0.9420	269.1
0.9479	0.9687	279.1

c. In 13.5-μm sintered stainless steel plate

x_1	y_1	P (mm Hg)
0.0488	0.3122	108.8
0.1510	0.5420	144.2
0.2948	0.6589	176.3
0.4259	0.7278	194.1
0.5517	0.7811	211.3
0.6888	0.8413	225.3
0.7980	0.8901	235.5
0.8441	0.9190	240.0
0.9100	0.9488	246.7
0.9499	0.9801	255.0

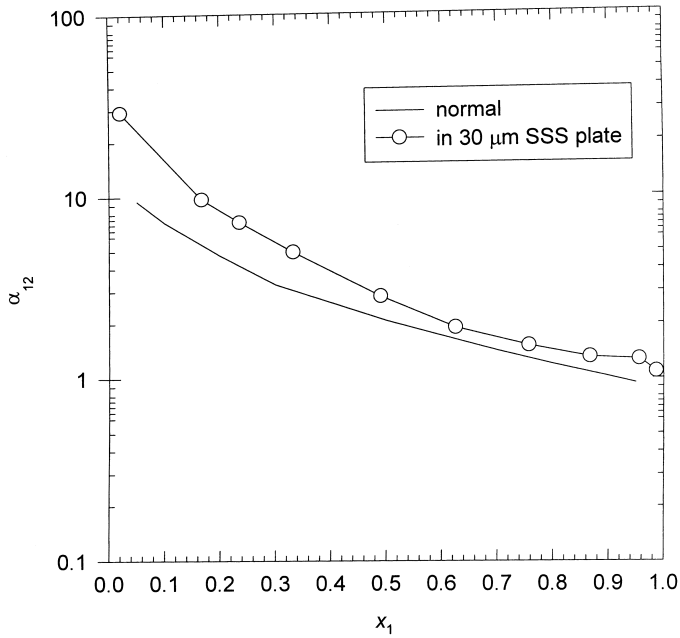

FIG. 3 Relative volatility of ethanol(1) with respect to water(2) at 323.15 K. The normal curve is from Ohe (14).

two liquids are not substantially altered even in the porous sintered stainless steel plate.

Experimental Activity Coefficients and Excess Gibbs Free Energy

The activity coefficients for VLE in porous media can be calculated by using Eq. (4) and the molar excess Gibbs free energy for the mixture in porous media can be calculated from Eq. (11). The resulting molar excess Gibbs free energy for the ethanol–water system in porous plates is shown in Fig. 4. This figure shows that the molar excess Gibbs free energy of the ethanol–water mixture in porous sintered stainless steel is substantially different from that for the normal (i.e., without porous plates) case. The change in $\tilde{G}^E$ from the normal is particularly evident in the intermediate concentration range, $0.30 \leq x_1 \leq 0.70$. On the other hand, for the ethanol–water system in porous carbon or Teflon plates, and for the acetone–ethanol system in any of the three porous plates, however, for the reasons mentioned above, there was no significant change in $\tilde{G}^E$.

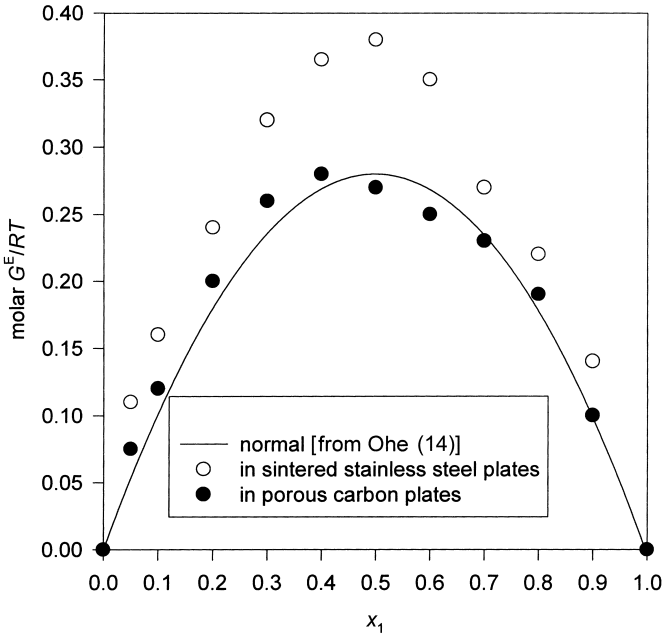

FIG. 4 Molar excess Gibbs free energy for ethanol–water system at 323.15 K.

Effect of Temperature on VLE

The effect of temperature on VLE was studied for the ethanol–water mixtures in the porous sintered stainless steel plate in the limited range of 323.15 to 333.15 K. The $x - y$ data for these temperatures is shown in Fig. 5 and does not show a significant effect in this range of temperatures, which is similar to the effect of temperature under normal conditions. However, a decrease in the activity coefficients was seen as the temperature increased. This also led to a slight decrease in $\tilde{G}^E$ with temperature.

Thermodynamic Consistency of the Experimental Data

The thermodynamic consistency of the measured VLE data of ethanol–water mixtures and acetone–ethanol mixtures was checked by the point-to-point method of Van Ness et al. (15), and the infinite dilution test of Kojima et al. (16) as modified by Jackson and Wilsak (17). A four-parameter Legendre polynomial was used for the excess Gibbs free energy. According to the Van Ness-Byer-Gibbs test (18), the VLE data are consistent if the mean absolute deviation between the measured and calculated va-

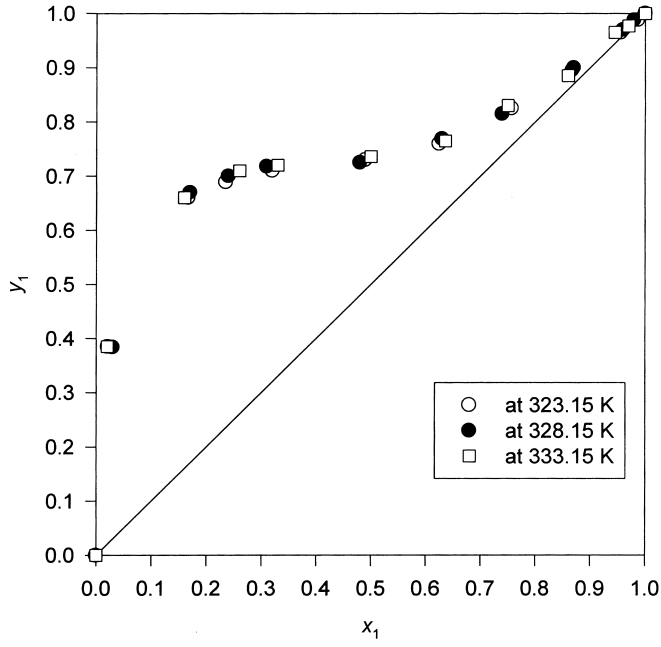

FIG. 5 Effect of temperature on $x_1 - y_1$ data for ethanol(1)–water(2) system in sintered porous stainless steel plate of 13.5-μm pore diameter.

por-phase mole fraction is less than 0.01. The experimental VLE data of this study, as shown in Table 5, were found to be thermodynamically consistent according to this test.

The infinite dilution test of Kojima-Jackson-Wilsak involves the calculation of the excess Gibbs free energy from the experimental data, and then the extrapolation to infinite dilution. A comparison is then to be made between these extrapolated values and those values obtained by extrapolating the ln γ_1 and ln γ_2 curves to infinite dilution. According to this test, the VLE data are consistent if the values agree within 30%. The experimental data of this study, as shown in Table 5, were also found to be thermodynamically consistent according to this test.

Correlation of the Experimental Data

The Wilson model, which is based on molecular considerations and whose adjustable parameters are related to the energies of interaction between the molecules, is used to correlate the activity-coefficients data, although other models may also be appropriate. The Wilson correlation is also useful for so-

TABLE 5
Thermodynamic Consistency Tests for the Experimental VLE Data for the Ethanol(1)–Water(2) System at 323.15 K and for the Acetone(1)–Ethanol(2) System at 305.15 K

System	Van Ness–Byer–Gibbs MAD (y)	Kojima–Jackson–Wilsak	
		Error for dilute component 1 (%)	Error for dilute component 2 (%)
Ethanol–water[a]	0.0097	10.8	8.4
Ethanol–water[b]	0.0084	14.1	6.6
Ethanol–water[c]	0.0081	16.5	7.6
Ethanol–water[d]	0.0093	11.8	8.9
Acetone–ethanol[a]	0.0087	11.4	9.4
Acetone–ethanol[b]	0.0100	10.4	8.1
Acetone–ethanol[c]	0.0096	11.3	9.6
Acetone–ethanol[d]	0.0083	14.4	7.1

[a] Normal.
[b] In sintered stainless steel plate of 13.5-μm pore diameter.
[c] In porous carbon plate of 30-μm pore diameter.
[d] In porous Teflon plate of 30-μmm pore diameter.

lutions of polar or associating components (e.g., alcohols) in nonpolar solvents, where other equations are not adequate (19–20).

This Wilson equation can be used to correlate the activity coefficients, γ_i^p. Then the total pressure, p^p, and the vapor phase composition, y_i^p, for a given liquid-phase composition can be predicted using Eq. (4), from the vapor pressure of the pure components. Defining the residuals $\delta y_i \equiv y_i^p - y_i$, and $\delta p \equiv p^p - p$, the objective is then to find the adjustable parameters in the Wilson equation that minimize $\sum(\delta y_i)^2$ and $\sum(\delta p_i)^2$. Van Ness and Abbott (21) showed that for the function to be used in data reduction, the following criterion should be achieved

$$\int_0^1 \frac{\delta y_1}{y_1 y_2}\, dx_1 = -\int_0^1 \ln \frac{\gamma_1}{\gamma_2}\, dx_1 \tag{27}$$

and if the data satisfy the Gibbs-Duhem equation, Eq. (27) should be equal to 0. Furthermore, they suggested that correlations that give scattered values of δy_i and δp around zero are likely to represent the VLE data well.

A computer program provided by Kyle (22), along with the infinite dilution activity coefficients, was used to find these parameters for the VLE of the systems studied, and the results are shown in Table 6. These parameters were used to predict the activity coefficients and then the vapor composition in the sintered stainless steel plate with 13.5-μm pore diameter as shown in Fig. 6.

TABLE 6
Wilson Parameters for the Ethanol(1)–Water(2) System at 323.15 K and for the Acetone(1)–Ethanol(2) System at 305.15 K

System	Λ_{12}	Λ_{21}
Ethanol–water[a]	0.21	0.83
Ethanol–water[b]	0.17	0.57
Ethanol–water[c]	0.18	0.85
Ethanol–water[d]	0.19	0.81
Acetone–ethanol[a]	0.33	0.98
Acetone–ethanol[b]	0.28	1.00
Acetone–ethanol[c]	0.32	0.99
Acetone–ethanol[d]	0.31	0.99

[a] Normal.
[b] In sintered stainless steel plate of 13.5-μm pore diameter.
[c] In porous carbon plate of 30-μm pore diameter.
[d] In porous Teflon plate of 30-μm pore diameter.

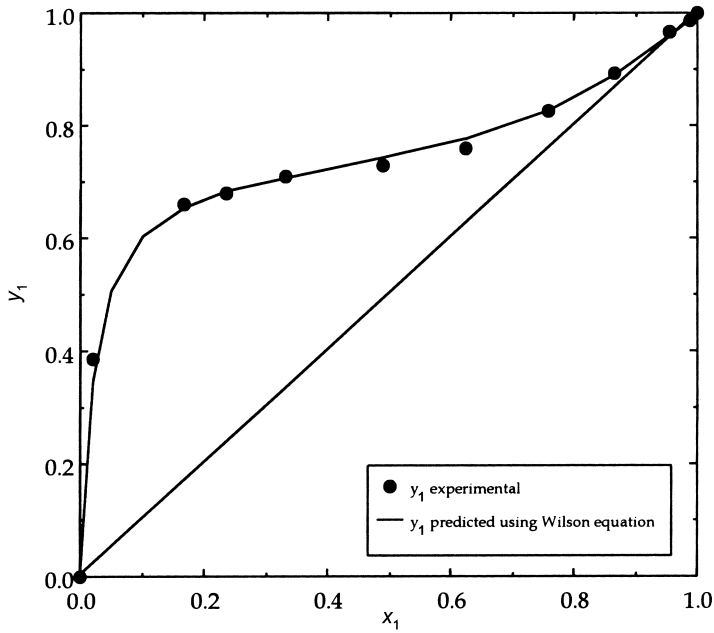

FIG. 6 Comparison between experimental and predicted VLE data using Wilson equation for ethanol(1)–water(2) system in sintered stainless steel plate of 13.5-μm pore diameter at 323.15 K.

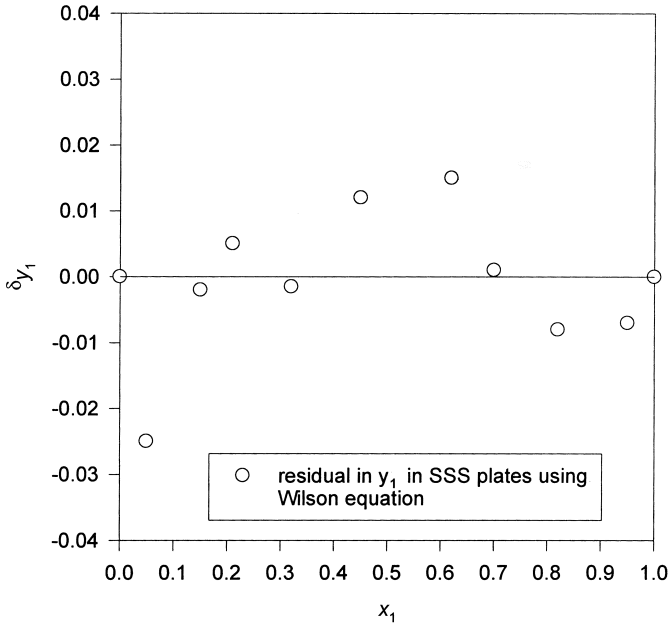

FIG. 7 Residuals in y_1 predicted for ethanol(1)–water(2) system at 323.15 K.

Figure 6 shows that the maximum error in predicting the vapor composition was 1.5% at low ethanol concentrations. However, at higher concentrations, the maximum error was less than 0.5%, which was within the experimental error. For the ethanol–water system in a porous carbon plate (not shown), the Wilson correlation predicted the VLE within 0.5% maximum error over the whole concentration range. These results were then used to calculate the residuals, and the results, as shown in Fig. 7, show that scattering of the residuals about zero is indeed obtained and $\int_0^1 \frac{\delta y_1}{y_1 y_2}\, dx_1 \cong 0$, implying that the Wilson equation can adequately correlate the VLE data of the ethanol–water system in porous plates.

CONCLUSIONS

The isothermal VLE data of two systems of different relative polarization in three different porous plates obtained using the static still show that porous plates can be used to alter the VLE of binary mixtures. The extent of alteration was found to be a function of the difference in the polarization of

the mixture components as well as the polarization of the solid. The experimental results for the ethanol–water system that possesses dissimilar component polarities show a significant alteration of its $x - y$ plot in porous sintered stainless steel plates, including a shift or elimination of the azeotrope. On the other hand, the $x - y$ plot of the ethanol–water system in porous plates of low polarization, as well as those for the acetone–ethanol system, possessing similar component polarization, in different porous plates show little variation.

ACKNOWLEDGMENT

The financial support provided by the Iowa Corn Promotion Board for this work is gratefully acknowledged.

NOTATION

a_i	activity coefficient of component $i = f_i/f_i^o$
$A^{\alpha\beta}$	molar interfacial area between phases α and β, m^2/mol
C	constant in vapor pressure equation, dimensionless
C^E	excess constant, $\equiv C - C_o$
f	fugacity
G	Gibbs energy, J
$\tilde{G}$	molar Gibbs energy, J/mol^{-1}
$\Delta\tilde{H}^E_{vl}$	excess molar enthalpy of vaporization due to presence of external fields, J/mol
K_i	distribution coefficient of component i
l	number of external fields
n	number of components
p	pressure, kPa; mm Hg
p_i^v	vapor pressure in the presence of external fields, kPa; mm Hg
$p_{i,o}^v$	vapor pressure in the absence of external fields, kPa; mm Hg
$\tilde{P}$	molar polarization, m^3/mol^{-1}
r	radius of curvature; pore radius, m
R	universal gas constant = 8.3143 J/mol^{-1} K^{-1}
S	entropy, J K^{-1}
$\tilde{S}$	molar entropy, J/mol^{-1} K^{-1}
T	temperature, K
V	volume, m^3
$\tilde{V}$	molar volume, $\equiv$ M/ρ, m^3/mol^{-1}
x_i^α	molar fraction of species i in phase α
x	vector of species molar fraction

Greek Letters

$\alpha_{1,2}$	relative volatility of component 1 with respect to component 2
δ	residual
ε	permittivity, $C^2\ J^{-1}/m^{-1}$
ε_r	relative permittivity, or dielectric constant, $\equiv \varepsilon/\varepsilon_0$
ε_0	permittivity of free space, $8.854 \times 10^{-12}\ C^2\ J^{-1}/m^{-1}$
φ_i	fugacity coefficient of *i* in the presence of external fields
γ_i	activity coefficient of the *i*th component in the presence of external fields
$\gamma_{i,o}$	activity coefficient of the *i*th component in the absence of external fields
ζ	extensive parameter conjugate with Ψ
K, κ_s	constants, dimensionless
μ_i^α	chemical potential of species *i* in phase α in the presence of external fields
$\mu_{i,o}^\alpha$	chemical potential of species *i* in phase α in the absence of external fields
π	number of phases
σ	surface energy or tension, mJ/m^{-2}, or mN/m^{-1}
ψ_i^α	generalized physicochemical potential of species *i* in phase α in the presence of external fields
Ψ	intensive parameter characterizing the external field

Subscripts

A	property at azeotropic point
F	property due to the external field
i	species *i*
L	London (dispersion) interactions
o	property in the absence of external fields
O	other interactions

Superscripts

E	excess thermodynamic property in presence of external fields
l	liquid phase
o	reference value
p	predicted
s	solid phase
v	vapor phase
∞	property with infinite radius of curvature, plane interface
$-$	partial molar thermodynamic property
~	molar thermodynamic property

Operations

$\otimes$ appropriate scalar product between Ψ and ζ

Abbreviations

VLE vapor–liquid equilibrium
SSS sintered stainless steel

REFERENCES

1. R. Rautenbach and R. Albrecht, *Membrane Processes*, Wiley, New York, 1989.
2. M. R. Ladisch and K. Dyck, "Dehydration of Ethanol: New Approach Gives Positive Energy Balance," *Science, 205*, 898 (1979).
3. J. Y. Lee, P. J. Westgate, and M. R. Ladisch, "Water and Ethanol Sorption Phenomena on Starch," *AIChE J., 37*, 1187 (1991).
4. G. C. Yeh, M. S. Shah, and B. V. Yeh, "Vapor-Liquid Equilibrium of Nonelectrolyte Solutions in Small Capillaries. 1. Experimental Determination of Equilibrium Composition," *Langmuir, 2*, 90 (1986).
5. G. C. Yeh, B. V. Yeh, B. J. Ratigan, S. J. Correnti, M. S. Yeh, D. W. Pitakowski, D. W. Fleming, D. B. Ritz, and J. A. Lariviere, "Separation of Liquid Mixtures by Capillary Distillation," *Desalination, 81*, 129–160 (1991).
6. G. C. Yeh, B. V. Yeh, S. T. Schmidt, M. S. Yeh, A. M. McCarthy, and W. J. Celenza, "Vapor–Liquid Equilibrium in Capillary Distillation," *Desalination, 81*, 161–187 (1991).
7. F. A. Abu Al-Rub, J. Akili, and R. Datta, "Distillation of Binary Mixtures with Capillary Porous Plates," *Sep. Sci. Technol., 33*, 1529–1550 (1998).
8. F. A. Abu Al-Rub and R. Datta, "Separation of 2-Propanol–Water Mixture with Capillary Porous Plates," *Ibid., 34*, 725–742 (1999).
9. F. A. Abu Al-Rub, and R. Datta, "Theoretical Study of Vapor Pressure of Pure Liquids in Porous Media," *Fluid Phase Equilibria, 147*, 65–83 (1998).
10. F. A. Abu Al-Rub, and R. Datta, "Theoretical Study of Vapor–Liquid Equilibrium Inside Capillary Porous Plates," *Ibid., 162*, 83–96 (1999).
11. N. S. J. Wong, "The Effects of Capillary Plates on Vapor–Liquid Equilibrium in Aqueous Alcohol Systems," *M.S. Thesis*, Dept. Chem. Eng., McGill University, Montreal, 1997.
12. F. A. Abu Al-Rub, "Distillation in Capillary Porous Media for Separation of Biomass Ethanol–Water Mixtures," *Ph.D. Thesis*, The University of Iowa, 1994.
13. J. A. Dean, *Lange's Handbook of Chemistry*, 14th ed., McGraw-Hill, New York, 1992.
14. S. Ohe, *Vapor–Liquid Equilibrium Data*, Elsevier, Amsterdam, 1989.
15. H. C. Van Ness, S. M. Byer, and R. E. Gibbs, "Vapor–Liquid Equilibrium. I. An Appraisal of Data Reduction Methods," *AIChE J., 19*, 238–244 (1973).
16. K. Kojima, H. M. Moon, and K. Ochi, "Thermodynamic Consistency Test of Vapor–Liquid Equilibrium Data" *Fluid Phase Equilibria, 56*, 269–284 (1990).
17. P. L. Jackson and R. A. Wilsak, "Thermodynamic Consistency Tests Based on the Gibbs-Duhem Equation Applied to Isothermal, Binary Vapor–Liquid Equilibrium Data: Data Evaluation and Model Testing of Vapor–Liquid Equilibrium Data," *Ibid., 103*, 105 (1995).
18. A. Fredenslund, J. Gmehling, and Rasumssen, *Vapor–Liquid Equilibrium Using UNIFAC*, Elsevier, Amsterdam, 1977.
19. J. M. Prausntiz, R. N. Lichtenthaler, and E. G. Azevedo, *Molecular Thermodynamics of Fluid-Phase Equilibrium*, 2nd ed., Prentice-Hall, Paramus, NJ, 1986.

20. G. M. Wilson, "Vapor–Liquid Equilibrium. XI. A New Expression for the Excess Free Energy of Mixing," *J. Am. Chem. Soc., 86*, 127 (1964).
21. H. C. Van Ness and N. M. Abbott, "Some Practical Consideration in Reduction of Vapor–Liquid Equilibrium Data," in *Chemical Engineering Thermodynamics*, (S. A. Newman, Ed.), Ann Arbor Sci., Ann Arbor, MI, 1983.
22. B. G. Kyle, *Chemical and Process Thermodynamics*, 2nd ed., Prentice Hall, Paramus, NJ, 1992.

Received by editor August 10, 1999
Revision received February 2000